

Further Insight into the Mechanism of Stereoselective Proton Abstraction by Bacterial Copper Amine Oxidase^{†,‡}

Masayasu Taki,^{§,||} Takeshi Murakawa,^{||,⊥,®} Takuya Nakamoto,[§] Mayumi Uchida,[§] Hideyuki Hayashi,[#] Katsuyuki Tanizawa,[⊥] Yukio Yamamoto,^{*,§} and Toshihide Okajima^{*,⊥}

Graduate School of Human and Environmental Studies, Kyoto University, Kyoto 606-8501, Japan, Institute of Scientific and Industrial Research, Osaka University, Ibaraki, Osaka 567-0047, Japan, and Department of Biochemistry, Osaka Medical College, Takatsuki, Osaka 569-8686, Japan

Received April 8, 2008

ABSTRACT: During the catalytic reaction of copper amine oxidase, one of the two prochiral hydrogen atoms at the C1 position of substrate amine is stereoselectively abstracted by a conserved Asp residue serving as a general base. Using stereospecifically deuterium-labeled enantiomers of 2-phenylethylamine, we previously showed that the *pro-S* α -proton is abstracted by the enzyme from *Arthrobacter globiformis* (AGAO) [Uchida, M., et al. (2003) *Biosci. Biotechnol. Biochem.* 67, 2664–2667]. More recently, we have also demonstrated that the *pro-S* selectivity of α -proton abstraction is fully retained even in the reaction of a mutant AGAO lacking the catalytic base [Chiu, Y.-C., et al. (2006) *Biochemistry* 45, 4105–4120]. On the basis of these findings, we have proposed that the stereoselectivity of α -proton abstraction is primarily determined by the conformation of the Schiff base intermediate formed between the substrate and the topa quinone cofactor (TPQ), stabilized by the binding of the distal part of the substrate to a hydrophobic pocket of the enzyme. In this conformation, the *pro-S* hydrogen atom to be abstracted is nearly perpendicular to the plane of the Schiff base–TPQ conjugate system, achieving the maximum overlap of σ - and π -orbitals. To further elucidate the stereochemical details, we have synthesized stereospecifically deuterium-labeled enantiomers of ethylamine, a very poor substrate for AGAO, in addition to those structurally related to the preferred substrate, 2-phenylethylamine. In marked contrast to the nearly complete *pro-S* selectivity of α -proton abstraction for most substrates that have been examined, the stereoselectivity for ethylamine decreased significantly to as little as 88%. The crystal structure of AGAO soaked with ethylamine showed very poor electron densities for the substrate Schiff base intermediate, showing that its conformation is not defined uniquely. Thus, the stereoselectivity of α -proton abstraction during the copper amine oxidase reaction is closely associated with the conformational flexibility of the substrate Schiff base intermediate.

Copper amine oxidases (CAOs,¹ EC 1.4.3.6) catalyze the oxidative deamination of various primary amines to the

corresponding aldehydes, coupled with the reduction of molecular oxygen to hydrogen peroxide (1–3). CAOs commonly contain a mononuclear copper ion and topa quinone (TPQ) as a redox-active organic cofactor in the active site of enzymes (4). The catalytic reaction of CAOs has been shown to proceed through a ping-pong mechanism consisting of two half-reactions (Scheme 1) (5). In the former reductive half-reaction, (i) the C5 carbonyl group of the oxidized cofactor (TPQ_{ox}) reacts with a substrate primary amine to form the substrate Schiff base (TPQ_{ssb}), (ii) the catalytic base, an invariant aspartic acid residue, then abstracts a proton at the substrate C1 position forming the product Schiff base (TPQ_{psb}), and (iii) TPQ_{psb} is then hydrolyzed to yield the first product aldehyde with concomitant reduction of the cofactor to the aminoresorcinol form (TPQ_{amr}). In the latter oxidative half-reaction, the reduced cofactor (TPQ_{amr}) is reoxidized by molecular oxygen to produce hydrogen peroxide and release ammonia by the following hydrolysis (6).

According to the previous stereochemical studies on abstraction of a proton from the C1 (α) position of substrate amine, the stereoselectivity depended on the enzyme source

[†] This study was supported by Grants-in-Aid for Scientific Research from the Japan Society for the Promotion of Science [Category B, Grants 14560066, 18370043, and 19350084 to T.O., K.T., and Y.Y., respectively; and Young Scientists (B), Grant 19750139 to M.T.].

[‡] The atomic coordinates and structure factors for the AGAO–ethylamine complex have been deposited in the Protein Data Bank (PDB) as entry 2ZL8.

* To whom correspondence should be addressed. T.O.: phone, +81-6-6879-4292; fax, +81-6-6879-8464; e-mail, tokajima@sanken.osaka-u.ac.jp. Y.Y.: phone and fax, +81-75-753-6833; e-mail, yamamoto_y@mbox.kudpc.kyoto-u.ac.jp.

[§] Kyoto University.

^{||} These authors contributed equally to this work.

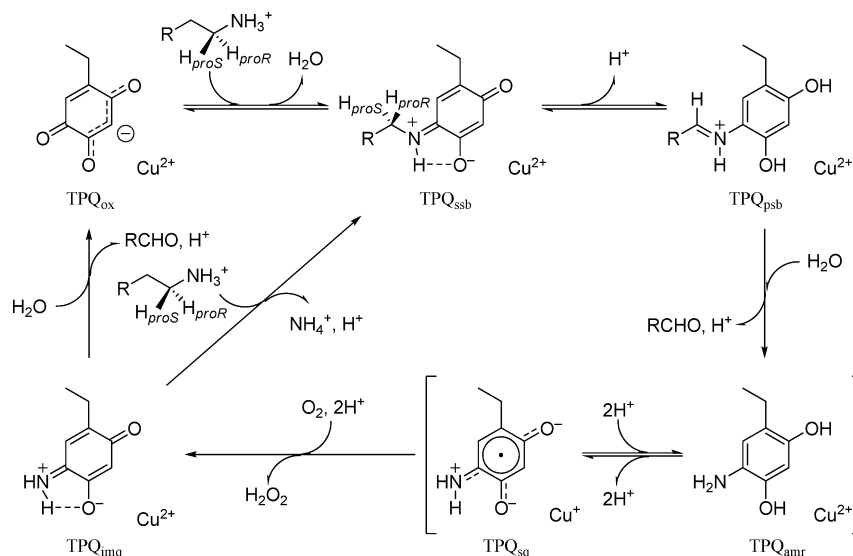
[⊥] Osaka University.

[®] Present address: Department of Biochemistry, Osaka Medical College, Takatsuki, Osaka 569-8686, Japan.

[#] Osaka Medical College.

¹ Abbreviations: AGAO, *Arthrobacter globiformis* phenylethylamine oxidase; CAO, copper amine oxidase; GC–MS, gas chromatography–mass spectrometry; HEPES, 2-[4-(2-hydroxyethyl)-1-piperidinyl]ethanesulfonic acid; 2-PEA, 2-phenylethylamine; TPQ, topa quinone; TPQ_{ssb}, substrate Schiff base of TPQ; TPQ_{psb}, product Schiff base of TPQ; TPQ_{ox}, oxidized form of TPQ; TPQ_{amr}, reduced aminoresorcinol form of TPQ.

Scheme 1: Reaction Mechanism of Copper Amine Oxidase



and the substrate that were used. For example, the *pro-S* α -proton of tyramine, dopamine, and benzylamine was abstracted in the reaction of the pea seedling enzyme, while the *pro-R* α -proton of tyramine and dopamine was abstracted in the reaction of the porcine plasma enzyme (7). On the other hand, the bovine plasma enzyme was non-stereoselective with tyramine and dopamine but *pro-S* selective with benzylamine, *p*-hydroxybenzylamine, and 3-methylbutylamine (7). We also reported the *pro-S* selectivity of α -proton abstraction during the oxidation of 2-phenylethylamine (2-PEA) by *Arthrobacter globiformis* phenylethylamine oxidase (AGAO) (8). In view of the highly conserved active-site structures of this class of enzymes (9–15), the origin of the inconsistent stereoselectivity of α -proton abstraction remains to be identified. We have recently determined the crystal structures of TPQ_{ssb} and TPQ_{psb} intermediates formed in a mutant enzyme of AGAO lacking the catalytic base (Asp298) but still showing a miniscule activity (16). Of the two prochiral α -hydrogen atoms generated in the final model of TPQ_{ssb}, the *pro-S* hydrogen is indeed oriented toward Ala298 (Asp298 in the wild-type enzyme) and located closer to Ala298 than the *pro-R* hydrogen, consistent with the stereoselectivity of AGAO described above. More importantly, however, in this conformation of TPQ_{ssb}, the *pro-S* hydrogen is nearly perpendicular to the plane of the Schiff base—TPQ ring so that the σ -orbital of the C α —H_S bond maximally overlaps with the π -orbital of TPQ_{ssb}. Furthermore, the *pro-S* selectivity of α -proton abstraction is completely retained even for the mutant enzyme without the catalytic base. These findings have led us to propose that the stereoselectivity of α -proton abstraction during the CAO reaction is primarily determined by the conformation of TPQ_{ssb}, rather than the geometry of the substrate relative to the catalytic base (16). Because the local region that binds or accommodates the distal part of the amine substrate (the opposite end from the amino group) is only poorly conserved among various CAOs (9–15), reflecting the difference in substrate specificity (1–3), the conformation of TPQ_{ssb} could vary depending on the enzyme and substrate that were used. We assume that this may be the reason for the inconsistent stereoselectivity of α -proton abstraction among various CAOs and substrates. To evaluate this hypothesis and gain further insight into the

mechanism of stereoselective α -proton abstraction, we have prepared stereospecifically deuterium-labeled enantiomers of tyramine, 2-(4-methoxyphenyl)ethylamine, 2-cyclohexylethylamine, and benzylamine, together with ethylamine, a very poor substrate for AGAO without an aromatic ring, and used them for stereochemical analyses of α -proton abstraction by AGAO. Interestingly, the *pro-S* selectivity decreased significantly only with ethylamine, for which AGAO has a very high K_m value. In addition, the crystal structure of the TPQ_{ssb} intermediate formed with ethylamine exhibited conformational ambiguity of the substrate Schiff base.

EXPERIMENTAL PROCEDURES

Instruments. ¹H NMR spectra were recorded on a JEOL JNM-EX-270 instrument at 270 MHz or a JEOL-alpha-500 instrument at 500 MHz. GC–MS analyses were carried out with Shimadzu GC-17A and GCMS-QP5050A instruments (starting column temperature of 50 °C, maintained for 5 min; increasing at a rate of 10 °C/min). A microspectrophotometer system for the single-crystal microscopy consisted of a deuterium tungsten halogen light (Ocean Optics, DT-MINI), Cassegrainian mirrors (Bunkoh-Keiki Co., Ltd.), an optical fiber, and a linear CCD-array spectrometer (Ocean Optics, SD2000).

Materials. AGAO was prepared in the Cu/TPQ-containing active form and assayed as described previously (6, 17). The enantiomeric pair of stereospecifically deuterium-labeled tyramines was synthesized according to the published protocols (18). Those of deuterium-labeled 2-(4-methoxyphenyl)ethylamine, 2-cyclohexylethylamine, and benzylamine were prepared as described in the Supporting Information. (S)-[1-²H]Ethanol was prepared as reported by Günther et al. (19). Silica gel C-200 (75–150 μ m, Wako) was used for column chromatography. Thin layer chromatography analysis was performed using Merck F254 silica gel-60 plates and viewed by UV light or developed with molybdo-phosphate.

Synthesis of (S)-[1-²H]Ethylamine. The procedures for the synthesis of deuterium-labeled ethylamines are shown in Scheme S1. (S)-[1-²H]Ethanol was first converted into benzyl ester by the Mitsunobu reaction (20), accompanied by the

inversion of configuration at the C1 position. Thus, a mixture of triphenylphosphine (17.7 g, 93 mmol), benzoic acid (8.2 g, 68 mmol), and diisopropyl azodicarboxylate (18.3 mL, 93 mmol) in THF (30 mL) was added to a solution of (*S*)-[1-²H]ethanol (3.0 g, 62 mmol) in THF (150 mL). The reaction mixture was stirred at room temperature under an Ar atmosphere for 4 days. After evaporation, the residue was purified by silica gel column chromatography (1:20 ethyl acetate/hexane mixture) to give (*R*)-[1-²H]ethyl benzoate (7.76 g, 83%): ¹H NMR (CDCl₃, 270 MHz) δ 1.38 (3H, dt, $J_H = 6.9$ Hz, $J_D = 1.0$ Hz, Me-CHD-), 4.36 (1H, qt, $J_H = 7.1$ Hz, $J_D = 1.6$ Hz, Me-CHD-), 7.39–7.44 (2H, m, Ar), 7.50–7.56 (1H, m, Ar), 8.02–8.06 (2H, m, Ar). *n*-Butyllithium (1.6 M in hexane, 28.9 mL, 46.3 mmol) was added dropwise at -50 °C to a solution of the (*R*)-[1-²H]ethyl benzoate (2.8 g, 18.5 mmol) in freshly distilled THF (28 mL), and the mixture was stirred for 3 h at the same temperature. *p*-Toluenesulfonyl chloride (8.8 g, 46.3 mmol) in dry THF (30 mL) was then added to the reaction mixture at -50 °C. After being kept in a refrigerator overnight, the mixture was poured into ice (60 g) and extracted with ether (4 \times 80 mL). The combined extracts were washed with brine and dried with MgSO₄. After evaporation, the residue was purified by silica gel column chromatography (1:10 ethyl acetate/hexane mixture) to give (*R*)-[1-²H]ethyl tosylate (3.29 g, 88%): ¹H NMR (CDCl₃, 270 MHz) δ 1.28 (3H, d, $J = 7.2$ Hz, Me-CHD-), 2.44 (3H, s, Ar-Me), 4.08 (1H, qt, $J_H = 7.0$ Hz, $J_D = 1.0$ Hz, Me-CHD-), 7.34 (2H, d, $J = 8.2$ Hz, Ar), 7.78 (2H, d, $J = 8.2$ Hz, Ar). The (*R*)-tosylate (3.29 g, 16.3 mmol) was added to a saturated ammonia solution in methanol (100 mL), and the mixture was stirred for 3 days at room temperature to give (*S*)-[1-²H]ethylamine *p*-toluenesulfonate salt (3.1 g, 87%), accompanied by the second inversion of configuration: ¹H NMR (D₂O, 270 MHz) δ 1.26 (3H, d, $J = 6.6$ Hz, Me-CHD-), 2.40 (3H, s, Ar-Me), 3.03 (1H, qt, $J_H = 7.2$ Hz, $J_D = 1.6$ Hz, Me-CHD-), 7.38 (2H, d, $J = 7.9$ Hz, Ar), 7.70 (2H, d, $J = 7.9$ Hz, Ar). Finally, (*S*)-[1-²H]ethylamine hydrogen bromide was obtained by dissolving (*S*)-[1-²H]ethylamine tosylate salt (746 mg, 3.4 mmol) in 5% NaOH (24 mL), extracting the mixture with ether (4 \times 20 mL), and adding hydrobromic acid (ca. 47%, 1 mL) to the combined extracts. Evaporation gave a white solid, and excess hydrobromic acid was removed by washing the mixture with ether.

Synthesis of (*R*)-[1-²H]Ethylamine. *p*-Toluenesulfonyl chloride (8.6 g, 45 mmol) was added to a solution of (*S*)-[1-²H]ethanol (1.2 g, 25 mmol) in pyridine (33 mL) at -30 °C. The reaction mixture was stored in a refrigerator overnight and then poured into ice (25 g). After the mixture had been stirred for 1 h, cold 4 M sulfuric acid (50 mL) was added. The mixture was extracted with ether (4 \times 80 mL), and the combined extracts were successively washed with ice-cold 0.5 M sulfuric acid, ice–water, ice-cold 5% NaOH, and again with ice–water. The organic layer was dried with MgSO₄, and the solvent was evaporated. The residue was purified by silica gel column chromatography (1:10 ethyl acetate/hexane mixture) to give (*S*)-[1-²H]ethyl tosylate (3.4 g, 67%): ¹H NMR (CDCl₃, 270 MHz) δ 1.28 (3H, d, $J = 7.2$ Hz, Me-CHD-), 2.44 (3H, s, Ar-Me), 4.08 (1H, qt, $J_H = 7.0$ Hz, $J_D = 1.0$ Hz, Me-CHD-N), 7.34 (2H, d, $J = 8.2$ Hz, Ar), 7.78 (2H, d, $J = 8.2$ Hz, Ar). As described for the (*R*)-enantiomer, the (*S*)-tosylate (2.0 g, 9.9 mmol) was converted

to (*R*)-[1-²H]ethylamine tosylate salt (1.77 g, 82%): ¹H NMR (D₂O, 270 MHz) δ 1.26 (3H, d, $J = 6.6$ Hz, Me-CHD-), 2.40 (3H, s, Ar-Me), 3.03 (1H, qt, $J_H = 7.2$ Hz, $J_D = 1.6$ Hz, Me-CHD-), 7.38 (2H, d, $J = 7.9$ Hz, Ar), 7.70 (2H, d, $J = 7.9$ Hz, Ar). The hydrogen bromide salt of (*R*)-[1-²H]ethylamine was also obtained as described above.

Determination of Enantiomeric Purity. Enantiomeric purities of the deuterium-labeled benzylamine and ethylamine were determined by ¹H NMR. To a suspension of amine hydrogen bromide salt (0.1 mmol) in CH₂Cl₂ (1 mL) were added successively triethylamine (30 μ L, 0.22 mmol) and (–)-camphanic chloride (24 mg, 0.11 mmol). After the mixture had been stirred at 0 °C for 3 h, saturated NaHCO₃ (2 mL) was added and the mixture was extracted with CH₂Cl₂ (3 \times 2 mL). The combined extracts were washed with brine and dried over MgSO₄. After evaporation, the residue was purified by preparative thin layer chromatography (1:2 ethyl acetate/hexane mixture) to give the corresponding labeled amide. ¹H NMR data for benzylamine (CDCl₃, 500 MHz): (*R*)-amide, δ 4.42–4.46 (1.00H, m, H_S), 4.51–4.55 (<0.030H, m, H_R); (*S*)-amide, 4.42–4.46 (<0.041H, m, H_R), 4.51–4.55 (1.00H, m, H_S). ¹H NMR data for ethylamine (C₆D₆, 500 MHz): (*R*)-amide, 2.85–2.92 (<0.008H, m, H_R), 3.03 (1.00H, qdt, $J_{vic} = 7.2$ Hz, $J_D = 1.8$ Hz, H_S); (*S*)-amide, 2.89 (1.00H, qdt, $J_{vic} = 7.2$ Hz, $J_D = 1.8$ Hz, H_R), 3.03–3.06 (<0.013H, m, H_S). The enantiomeric purities of the deuterium-labeled amines were calculated from the integral ratio of the two protons.

Determination of Stereoselectivity of α -Proton Abstraction. The reaction mixture (1 mL) containing 0.2–0.5 mM substrate amine and an appropriate amount of AGAO (0.6, 0.8, 12.5, and 490 μ g for tyramine, 2-cyclohexylethylamine, benzylamine, and ethylamine, respectively) in 200 mM HEPES buffer (pH 6.8) was incubated at room temperature for 2 h. Except for ethylamine, each aldehyde product was extracted with ethyl acetate (0.5 mL) and then directly analyzed by GC–MS. For ethylamine, 2,4-dinitrophenylhydrazine (2.5 mg, 12 μ mol) in 3 M HCl (1 mL) was added to the incubated solution. The hydrazone of acetaldehyde thus formed was extracted with ethyl acetate (0.5 mL) and then analyzed by GC–MS. In all cases, the deuterium contents of the products were determined by the mass number of the molecular ion peaks and the peak intensities, which were rectified with the concomitant *M* – 1 and *M* + 1 peaks observed for the nonlabeled aldehydes. The deuterium contents of the substrate amine were also determined by the same method using GC–MS.

X-ray Crystallographic Analysis. The purified AGAO was crystallized by the microdialysis method as described previously (6); the protein solution (10 mg/mL) was placed in a 50 μ L dialysis button and dialyzed at 16 °C against 1.05 M potassium-sodium tartrate in 25 mM HEPES buffer (pH 6.8). After sufficient growth of the crystals, the dialysis button was transferred into the new reservoir solution supplemented with 45% (v/v) glycerol as a cryoprotectant and kept at 16 °C for 24 h. For determination of the crystal structures of the catalytic intermediate generated in the active site, the crystal was further soaked at 16 °C for 2 min in the new reservoir solution containing 45% (v/v) glycerol and 300 mM ethylamine. The crystals were mounted on thin nylon loops (ϕ , 0.4–0.5 mm) and frozen by being flash-cooled to 100 K in a cold N₂ gas stream. Before exposure to X-rays, the

Table 1: Statistics of Data Collection and Crystallographic Refinement for the AGAO–Ethylamine Complex

Data Collection	
temperature (K)	100
wavelength (Å)	0.9
space group	<i>I</i> 2
unit cell dimensions	
<i>a</i> , <i>b</i> , <i>c</i> (Å)	157.76, 63.52, 184.07
β (deg)	111.90
no. of observations	657713
no. of unique reflections	172009
<i>d</i> _{max} – <i>d</i> _{min} (Å)	70.0–1.73
<i>I</i> / <i>σ</i> <i>I</i>	4.6
redundancy	3.7
overall completeness (%)	97.6
overall <i>R</i> _{merge} (%) ^a	7.6
Refinement Statistics	
<i>d</i> _{max} – <i>d</i> _{min} (Å)	40.0–1.73
residues in the core <i>φφ</i> region (%)	87.6
no. of solvent atoms	1203
rms deviation from ideal values	
bond lengths (Å)	0.005
bond angles (deg)	1.37
residual <i>R</i> (%) ^b	19.2
residual <i>R</i> _{free} (%) ^c	21.3
fraction of data in the <i>R</i> _{free} set (%)	5

^a $R_{\text{merge}} = \sum_i \sum_h |I_{h,i} - \langle I_h \rangle| / \sum_h \sum_i I_{h,i}$, where $I_{h,i}$ is the intensity value of the i th measurement of h and $\langle I_h \rangle$ is the corresponding mean value of I_h for all i measurements. ^b $R = \sum ||F_o| - |F_c|| / \sum |F_o|$. ^c R_{free} is an *R* factor of the CNS refinement evaluated for 5% of the reflections that were excluded from the refinement.

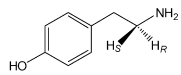
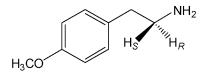
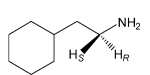
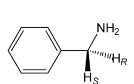
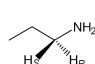
crystal was analyzed by single-crystal spectroscopy at 100 K to confirm the formation of the ethylamine–TPQ complex. The absorption spectrum was recorded in the wavelength region of 178–879 nm and corrected for the air blank baseline and dark reference.

Diffraction data sets were collected at 100 K with synchrotron X-radiation ($\lambda = 0.9$ Å) using an imaging plate, DIP6040 (Bruker AXS, Madison, WI), in station BL44XU at SPring-8 (Hyogo, Japan). The collected data were processed and scaled using MOSFLM (21) and SCALA (22), respectively. Refinements, calculation of the electron density map, and assignment of solvent molecules were performed using CNS version 1.1 (23). Manual rebuilding was performed using an xfit module in XtalView (24). The wild-type AGAO structure (Protein Data Bank entry 1IU7) without solvent molecules was used as an initial model with TPQ382 being replaced with an unmodified Tyr residue. The model of the catalytic intermediate was built using Insight II (Accelrys), and then the topology and parameter file used for the CNS refinement was generated with XPLO2D in X-UTIL (25). The details and statistics of data collection and refinement are summarized in Table 1.

RESULTS AND DISCUSSION

Preparation of Stereospecifically Deuterium-Labeled Substrates. To investigate whether the substrate-dependent stereochemical variation of α -proton abstraction, reported for bovine plasma CAO (7), is also observed with AGAO, we prepared several stereospecifically deuterium-labeled amines structurally related to 2-PEA: tyramine, 2-(4-methoxyphenyl)ethylamine, 2-cyclohexylethylamine, and benzylamine, as well as ethylamine, a small amine without an aromatic ring (Table 2). Except for the arduous syntheses

Table 2: Synthesized Deuterium-Labeled Amines

amine	label	ee (%) ^a
tyramine	 (R)-[1- ² H] (S)-[1- ² H]	100 100
2-(4-methoxyphenyl)ethylamine	 (R)-[1- ² H] (S)-[1- ² H]	100 100
2-cyclohexylethylamine	 (R)-[1- ² H] (S)-[1- ² H]	100 100
benzylamine	 (R)-[1- ² H] (S)-[1- ² H]	94 92
ethylamine	 (R)-[1- ² H] (S)-[1- ² H]	> 99 > 99

^a Enantiomeric excess (ee) was determined for benzylamine and ethylamine by ¹H NMR of the amide with (–)-camphoric acid. The ee values of the other amines were regarded as 100% on the basis of the starting materials.

of the deuterium-labeled enantiomers of ethylamine described in detail in Experimental Procedures, those of the other amines are given in the Supporting Information. Briefly, the deuterium-labeled enantiomers of 2-(4-methoxyphenyl)ethylamine were prepared using tyrosine decarboxylase as reported for the synthesis of deuterium-labeled tyramine (18). Chirally labeled 2-cyclohexylethylamines were synthesized from the corresponding labeled 2-PEA via hydrogenation with a rhodium catalyst in acetic acid. Chirally labeled benzylamines were prepared by successive mesylation and amination of (S)- and (R)-[1-²H]benzyl alcohols, which were obtained by the asymmetric reduction of deuterated benzaldehyde with (R)- and (S)-alpine boranes, respectively (26). Structures and enantiomeric purities of these chirally labeled amines that were synthesized are summarized in Table 2. Furthermore, stereospecifically deuterium-labeled enantiomers of ethylamine with very high deuterium contents and enantiomeric purities (Tables 2 and 4) were both synthesized from (S)-[1-²H]ethanol, according to the procedures shown in Scheme S1.

Substrate Specificity. Prior to conducting the stereochemical studies, we performed steady-state kinetic analysis to determine the substrate specificity of AGAO using the five amine substrates listed in Table 2, but without deuterium labeling. As summarized in Table 3, K_m and k_{cat} values for tyramine and 2-(4-methoxyphenyl)ethylamine were comparable with those for 2-PEA previously determined at 30 °C ($K_m = 2.5 \pm 0.025$ μM , $k_{\text{cat}} = 76 \pm 0.76$ s^{-1} , and $k_{\text{cat}}/K_m = 30$ $\mu\text{M}^{-1} \text{s}^{-1}$) (16). In marked contrast, the values for 2-cyclohexylethylamine and benzylamine were much higher for K_m and lower for k_{cat} than those for 2-PEA. These results show that a benzene ring and two methylene carbons are required for amines to be an efficient substrate of AGAO. Furthermore, the K_m value for ethylamine was approximately 7×10^4 -fold higher than that for 2-PEA, even though the k_{cat} value was on the same order of magnitude as that for 2-cyclohexylethylamine. The high K_m value for ethylamine cannot be explained by an approximately 10-fold difference in the concentrations of deprotonated forms of the amines in the assay mixture (pH 6.8), as estimated from their pK_a

Table 3: Steady-State Kinetic Parameters of AGAO^a

	K_m (μ M)	k_{cat} (s^{-1})	k_{cat}/K_m (μ M ⁻¹ s ⁻¹)
tyramine	10.4 \pm 1.5	35 \pm 1.0	3.4 \pm 0.6
2-(4-methoxyphenyl)ethylamine	11.9 \pm 1.3	30 \pm 1.0	2.5 \pm 0.4
2-cyclohexylethylamine	360 \pm 10	4.0 \pm 0.1	(1.1 \pm 0.1) $\times 10^{-2}$
benzylamine	100 \pm 8	0.24 \pm 0.01	(2.4 \pm 0.3) $\times 10^{-3}$
ethylamine	(1.70 \pm 0.27) $\times 10^5$	1.00 \pm 0.06	(5.9 \pm 1.5) $\times 10^{-6}$

^a Determined at 15 °C (except for that of 2-cyclohexylethylamine, for which the assays were conducted at 25 °C) by systematically changing the concentration of substrates with an atmospheric O₂ concentration (16). The kinetic data were fitted to the Michaelis–Menten equation by nonlinear regression using Kaleidagraph version 3.0 (Abelbeck Software).

Table 4: Oxidation of Deuterium-Labeled Ethylamine by AGAO

substrate ethylamine	relative peak intensity of the product hydrazone ^b				R = NHC ₆ H ₃ (NO ₂) ₂ , major component (%) ^d	stereoselectivity
	m/z 223	m/z 224	m/z 225	m/z 226		
unlabeled	0.001	1.000 ^c	0.134	—	—	—
(<i>S</i>)-[1- ² H] ^a	0.053	1.000 ^c	0.319	—	CH ₃ CH=NR (88 \pm 3)	² H retention, 12%
(<i>R</i>)-[1- ² H] ^a	—	0.140	1.000 ^c	0.135	CH ₃ CD=NR (88 \pm 2)	H abstraction, 88%

^a Deuterium contents were determined to be >99% by ¹H NMR. ^b 2,4-Dinitrophenylhydrazone of acetaldehyde. ^c Molecular ion peak, M⁺. ^d Percent contents of the major component shown in parentheses were calculated from the mass number of the molecular ion peak and the peak intensity, which was rectified with the concomitant M – 1 and M + 1 peaks.

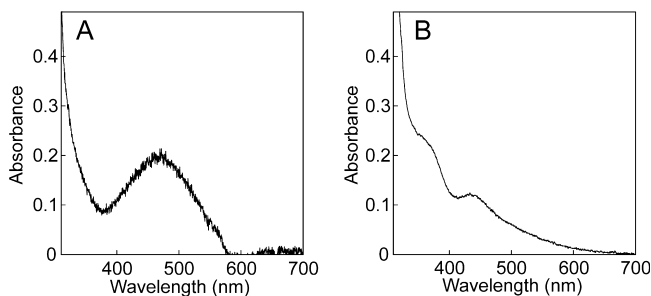


FIGURE 1: UV–vis absorption spectra of AGAO crystals. (A) Spectrum of a substrate-free AGAO crystal. (B) Spectrum of the AGAO crystal after it had been soaked with ethylamine for 2 min.

values (2-PEA, ~9.8; ethylamine, ~10.8); substrate amines must be deprotonated to attack the C5=O group of TPQ in the reductive half-reaction (5). Thus, it is suggested that AGAO scarcely forms a Michaelis complex with a small amine without a benzene ring. Collectively, tight binding of the distal part (an aromatic ring) of substrate to a hydrophobic pocket of the enzyme plays an important role in the catalytic reaction of AGAO, as discussed later.

Stereoselectivity of α -Proton Abstraction. In the reductive half-reaction of CAOs, either of the two prochiral α -protons, *pro-R* or *pro-S*, of substrate amine is abstracted from TPQ_{ssb} by a conserved catalytic base (Asp298 in AGAO) (16). The stereoselectivity of α -proton abstraction by AGAO, which showed the *pro-S* specificity with 2-PEA as the substrate (8), was further investigated using several chirally labeled amines (Table 2). The deuterium contents in the product aldehydes were directly analyzed by GC–MS (except for acetaldehyde produced from ethylamine, vide infra) and calculated from the relative intensities of the molecular ions, which were rectified with the concomitant M – 1 and M + 1 peaks observed for the nonlabeled samples. The major ion peak of the product aldehyde from (*S*)-[1-²H]tyramine was found at the same position (m/z 136) with the product from the nonlabeled tyramine, indicating that the deuterium label was lost almost completely (>99%) during the oxidation reaction by AGAO (see Table S1 of the Supporting Information). In the complementary experiment with (*R*)-[1-²H]tyramine, the label was retained nearly completely

(>99%) in the product aldehyde detected in the major ion peak at m/z 137 (Table S1). Similar results were obtained with stereospecifically deuterium-labeled enantiomers of 2-(4-methoxyphenyl)ethylamine, 2-cyclohexylamine, and benzylamine (Tables S2–S4, respectively). Altogether, AGAO exhibits nearly complete stereoselectivity for the *pro-S* α -proton irrespective of the amine substrates used, unlike the bovine plasma enzyme (7).

After successful syntheses of chirally labeled enantiomers of ethylamine possessing >99% enantiomeric purities, we further pursued the stereochemical studies with ethylamine, a very poor substrate for AGAO as described above. In this case, the volatile product, acetaldehyde, which was hardly detected by the direct GC–MS analysis, was therefore converted in situ into the corresponding 2,4-dinitrophenylhydrazone. With (*S*)-[1-²H]ethylamine as the substrate, a molecular ion peak at 224 Da, corresponding to the hydrazone of acetaldehyde containing no deuterium atom, was detected as the major product (Table 4). However, a significant intensity of the neighboring M + 1 peak, corresponding to the product hydrazone containing a deuterium atom (225 Da), was also observed, indicating some retention of the deuterium label. Surprisingly, the deuterium content in the product hydrazone was calculated to be not less than 12% from the peak intensity after correction with the concomitant M – 1 and M + 1 peaks observed for the nonlabeled samples. The complementary experiment using (*R*)-[1-²H]ethylamine as a substrate also showed that not more than 88% of the original deuterium was retained in the product hydrazone with a molecular ion peak at 225 Da. Thus, these results clearly show that AGAO exhibits an incomplete stereoselectivity (88%) of α -proton abstraction in the case of ethylamine. This contrasts markedly with the nearly complete *pro-S* stereoselectivity for the aforementioned amine substrates with a bulky group at the distal position.

X-ray Crystal Structure of the Catalytic Intermediate. To gain structural insight into the incomplete stereospecificity of α -proton abstraction exclusively observed for ethylamine, an X-ray crystal structure of the catalytic intermediate has been determined using ethylamine as the substrate. Although

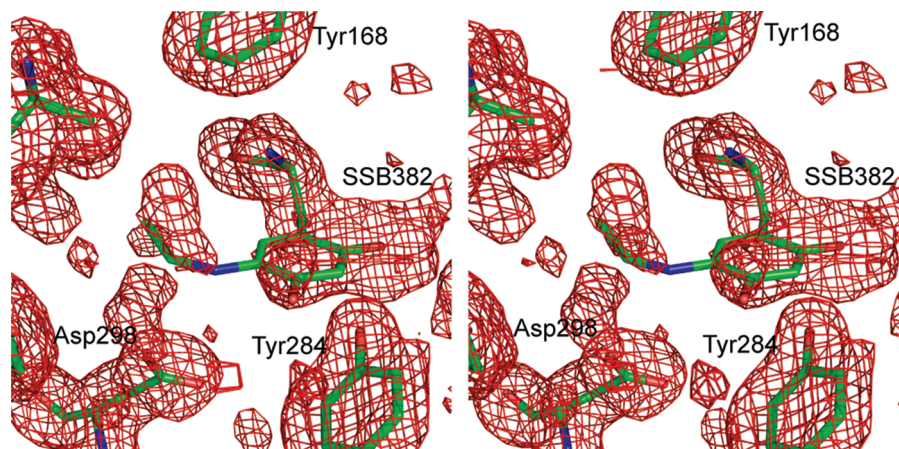


FIGURE 2: Stereoview of the active site structure of AGAO/ethylamine. The annealed $F_o - F_c$ omit map was contoured at 2.8σ and is shown with red mesh.

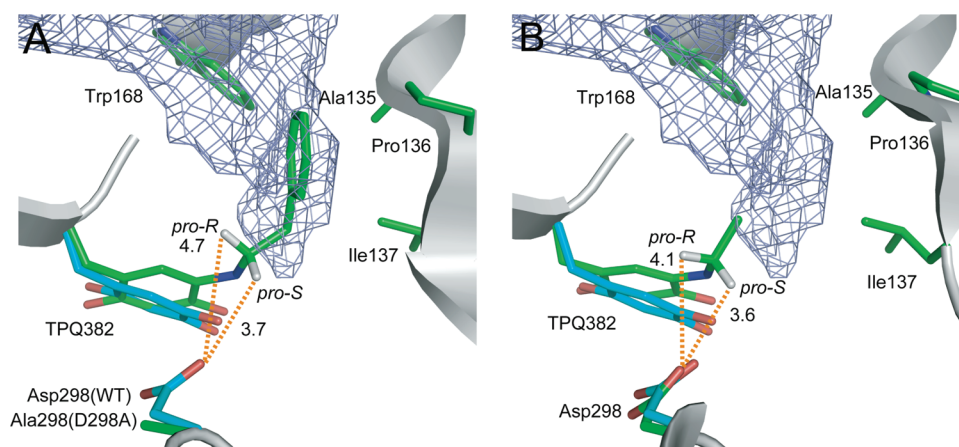


FIGURE 3: Comparison of the 2-PEA- and ethylamine-derived TPQ_{ssb} structures. (A) Model of 2-PEA-derived TPQ_{ssb} in the D298A mutant (green stick) superimposed with that of TPQ_{ox} in the substrate-free AGAO (blue stick). (B) Model of ethylamine-derived TPQ_{ssb} (green stick) superimposed with that of TPQ_{ox} in the substrate-free AGAO (blue stick). The distances between the computer-generated prochiral α -hydrogen atoms and the closest oxygen atom of the carboxyl group of Asp298 (superimposed in panel A) are shown in angstroms. The hydrophobic cavity involved in binding of the distal part of the substrate was generated with VOIDOO (28) mostly using default parameters and is drawn with gray mesh.

the K_m value for ethylamine is very high (170 mM), the k_{cat} value is not so low (3.0 s^{-1}) (Table 3). Therefore, it was expected that the oxidation reaction of ethylamine would proceed rather swiftly in the AGAO crystals. Thus, an AGAO crystal was soaked with 300 mM ethylamine for 2 min and then immediately frozen by being flash-cooled to 100 K in a cold N_2 gas stream; this crystal is hereafter termed AGAO/ethylamine. Before being exposed to X-rays, AGAO/ethylamine was subjected to single-crystal microspectrophotometry at 100 K for spectral identification of reaction intermediates that formed, if any, in the crystal. The AGAO/ethylamine crystal exhibited a UV-vis spectrum different from that of the substrate-free AGAO crystals (Figure 1) but rather similar to that of the TPQ_{ssb} intermediate formed during the reaction with 2-PEA or tyramine (16, 27). This clearly shows that the catalytic reaction has proceeded in the crystal and the TPQ_{ssb} intermediate has been successfully freeze-trapped after being soaked with the crystal for 2 min with ethylamine.

The structure of AGAO/ethylamine was determined by X-ray crystallography to 1.73 Å resolution. The refined structure gave an R factor of 0.19 and an R_{free} of 0.21 (Table 1). The overall structure of AGAO/ethylamine was almost identical with those of the substrate-free AGAO (PDB entry

1IU7) (6) and the 2-PEA-derived TPQ_{ssb} intermediate formed in the D298A mutant of AGAO (PDB entry 2CWU) (16), with root-mean-square deviations for main chain atoms of 0.39 and 0.24 Å, respectively. A small but obvious difference was observed only in the active site. Although the electron densities of TPQ_{ssb} and TPQ_{psb} formed in the D298A crystals had been very clearly observed in an annealed $F_o - F_c$ omit map contoured at 2.8σ (16), those corresponding to the catalytic intermediate (TPQ_{ssb}) formed from ethylamine were extremely low in the $F_o - F_c$ omit map drawn at the same contour level, particularly in contrast to the very clear electron densities for the surrounding residues (Figure 2). More specifically, the electron density around the C5–C6 edge of the modeled TPQ ring was poorer than that of the other part of the ring, indicating that the ethylamine moiety of TPQ_{ssb} has virtually no fixed conformation. These data provide strong evidence for the ethylamine-derived TPQ_{ssb} intermediate having a highly flexible conformation in the AGAO/ethylamine crystal. The conformational flexibility of the ethylamine-derived TPQ_{ssb} is most likely due to the absence of binding of the distal part of substrate to the local hydrophobic cavity of the enzyme, as described later, which could also be a cause for the high K_m of AGAO for ethylamine and would eventually lead to the incomplete

stereoselectivity of α -proton abstraction. Nevertheless, we have tentatively modeled TPQ_{ssb} so that the electron densities best accommodate the TPQ ring (Figure 2). In this model, the TPQ ring is tilted upward at the C5–C6 edge with the ring angle of $\sim 18^\circ$ relative to that of substrate-free AGAO (see Figure 3B), which also supports the idea that it is not free TPQ but TPQ_{ssb} (16).

Comparison of 2-PEA- and Ethylamine-Derived TPQ_{ssb} Structures. Shown in Figure 3 are the structures of the 2-PEA-derived TPQ_{ssb} determined previously with the D298A mutant of AGAO (16) and the ethylamine-derived TPQ_{ssb} determined here with the wild-type enzyme (AGAO/ethylamine). Although hydrogen atoms generally cannot be detected by X-ray crystallography, their coordinates, particularly those connected to carbon atoms, can be calculated using known bond distances and angles. The two prochiral α -hydrogen atoms of substrate were thus generated in the final models of the 2-PEA-derived and ethylamine-derived TPQ_{ssb} intermediates (Figure 3). In the 2-PEA-derived TPQ_{ssb} structure (16), it is evident that the *pro-S* hydrogen is positioned more perpendicular (dihedral angle defined by CD2, CE2, C1, and *pro-S* hydrogen atoms of 87°) to the plane of the Schiff base–TPQ ring π -electron system than the *pro-R* hydrogen (-22°) and also is oriented toward Ala298, which is almost superimposable with Asp298 in the wild-type enzyme. The distance to one of the two carboxyl oxygen atoms of the superimposed Asp298 is shorter by ~ 1.0 Å for the *pro-S* hydrogen than for the *pro-R* hydrogen (Figure 3A). In the ethylamine-derived TPQ_{ssb} structure (Figure 3B), the *pro-S* hydrogen is positioned less perpendicularly (64°) with respect to the Schiff base–TPQ plane, and the difference in the distances between the two prochiral hydrogen atoms and the carboxyl oxygen is considerably smaller (~ 0.5 Å) than in 2-PEA-derived TPQ_{ssb}. Altogether, these structural features of the *pro-S* hydrogen atom in the TPQ_{ssb} intermediate are presumably the main reason for the lowered stereoselectivity of α -proton abstraction with ethylamine. The conformational flexibility of ethylamine-derived TPQ_{ssb} would further decrease the degree of stereochemical discrimination between the *pro-S* and *pro-R* hydrogen atoms.

In the 2-PEA-derived TPQ_{ssb} structure, the distal part (benzene ring) of substrate 2-PEA is well accommodated within the hydrophobic cavity of the enzyme (Figure 3A), located at the bottom of the funnel-shaped substrate channel (11), thereby affording a fixed conformation of TPQ_{ssb} (16). Clearly, the ethyl group of ethylamine-derived TPQ_{ssb} is too small to interact sufficiently with the hydrophobic cavity (Figure 3B). The absence of such hydrophobic interaction at the distal end of the substrate most probably leads to the conformational flexibility of the TPQ_{ssb} intermediate.

Concluding Remarks. We have recently reported that the step of stereospecific α -proton abstraction by AGAO is largely driven by quantum mechanical hydrogen tunneling rather than the classical transition-state mechanism (27). Furthermore, X-ray crystallographic structures of the reaction intermediates (TPQ_{ssb}) formed from 2-PEA and tyramine revealed a small difference in the binding mode of the distal parts of substrates, which would modulate hydrogen tunneling proceeding through either active or passive dynamics. Collectively, the hydrophobic cavity involved in binding of the distal part of the substrate plays extremely important roles in the AGAO catalysis, providing tight binding for preferred

substrates with an aromatic ring, thereby restricting the conformational flexibility of the reaction intermediates (TPQ_{ssb} and TPQ_{psb}) in performing efficient and stereospecific α -proton abstraction, and modulating the mode of hydrogen tunneling. The substrate-binding hydrophobic cavity of AGAO consists of the side chains of Phe105, Ala135, Pro136, Leu137, Trp168, Tyr302, Tyr307, Ile379, Phe407, Leu358, and Trp359, most of which are less conserved among various CAOs (9–15). Therefore, this region could also account for the significant difference in the substrate specificities of various CAOs as well as the substrate- and enzyme-dependent stereochemical variation of α -proton abstraction by forming different conformations of TPQ_{ssb}.

ACKNOWLEDGMENT

We thank Y. Kawano (RIKEN Harima Institute, Japan) for allowing to use of the microspectrophotometer system for single-crystal microscopy. The radiation experiment was done at the BL44XU in SPring-8 with the approval of the Japan Synchrotron Radiation Research Institute (JASRI) (Proposal No. 2005A6706).

SUPPORTING INFORMATION AVAILABLE

Descriptions of the synthetic procedures for chirally labeled amines and tables of the results of oxidation by AGAO (besides those for enantiomers of ethylamine). This material is available free of charge via the Internet at <http://pubs.acs.org>.

REFERENCES

- MacIntire, W. S., and Hartmann, C. (1993) Copper-containing amine oxidase. In *Principles and Applications of Quinoproteins* (Davidson, V. L., Ed.) pp 97–171, Marcel Dekker, New York.
- Klinman, J. P., and Mu, D. (1994) Quinonozymes in biology. *Annu. Rev. Biochem.* 63, 299–344.
- Knowles, P. F., and Dooley, D. M. (1994) Amine oxidases. *Metal Ions in Biological Systems*, Vol. 30, pp 361–403, Marcel Dekker, New York.
- Janes, S. M., Mu, D., Wemmer, D., Smith, A. J., Kaur, S., Maltby, D., Burlingame, A. L., and Klinman, J. P. (1990) A new redox cofactor in eukaryotic enzymes: 6-Hydroxydopa at the active site of bovine serum amine oxidase. *Science* 248, 981–987.
- Mure, M., Mills, S. A., and Klinman, J. P. (2002) Catalytic mechanism of the topa quinone containing copper amine oxidases. *Biochemistry* 41, 9269–9278.
- Kishishita, S., Okajima, T., Kim, M., Yamaguchi, H., Hirota, S., Suzuki, S., Kuroda, S., Tanizawa, K., and Mure, M. (2003) Role of copper ion in bacterial copper amine oxidase: Spectroscopic and crystallographic studies of metal-substituted enzymes. *J. Am. Chem. Soc.* 125, 1041–1055.
- Coleman, A. A., Hindsgaul, O., and Palcic, M. M. (1989) Stereochemistry of copper amine oxidase reactions. *J. Biol. Chem.* 264, 19500–19505.
- Uchida, M., Ohtani, A., Kohyama, N., Okajima, T., Tanizawa, K., and Yamamoto, Y. (2003) Stereochemistry of 2-phenylethylamine oxidation catalyzed by bacterial copper amine oxidase. *Biosci. Biotechnol. Biochem.* 67, 2664–2667.
- Parsons, M. R., Convery, M. A., Wilmot, C. M., Yadav, K. D., Blakeley, V., Corner, A. S., Phillips, S. E., McPherson, M. J., and Knowles, P. F. (1995) Crystal structure of a quinoenzyme: Copper amine oxidase of *Escherichia coli* at 2 Å resolution. *Structure* 3, 1171–1184.
- Kumar, V., Dooley, D. M., Freeman, H. C., Guss, J. M., Harvey, I., McGuirl, M. A., Wilce, M. C., and Zubak, V. M. (1996) Crystal structure of a eukaryotic (pea seedling) copper-containing amine oxidase at 2.2 Å resolution. *Structure* 4, 943–955.
- Wilce, M. C. J., Dooley, D. M., Freeman, H. C., Guss, J. M., Matsunami, H., McIntire, W. S., Ruggiero, C. E., Tanizawa, K., and Yamaguchi, H. (1997) Crystal structures of the copper-

- containing amine oxidase from *Arthrobacter globiformis* in the holo and apo forms: Implications for the biogenesis of topaquinone. *Biochemistry* 36, 16116–16133.
12. Li, R., Klinman, J. P., and Mathews, F. S. (1998) Copper amine oxidase from *Hansenula polymorpha*: The crystal structure determined at 2.4 Å resolution reveals the active conformation. *Structure* 6, 293–307.
 13. Duff, A. P., Cohen, A. E., Ellis, P. J., Kuchar, J. A., Langley, D. B., Shepard, E. M., Dooley, D. M., Freeman, H. C., and Guss, J. M. (2003) The crystal structure of *Pichia pastoris* lysyl oxidase. *Biochemistry* 42, 15148–15157.
 14. Lunelli, M., Di Paolo, M. L., Biadene, M., Calderone, V., Battistutta, R., Scarpa, M., Rigo, A., and Zanotti, G. (2005) Crystal structure of amine oxidase from bovine serum. *J. Mol. Biol.* 346, 991–1004.
 15. Airenne, T. T., Nymalm, Y., Kidron, H., Smith, D. J., Pihlavisto, M., Salmi, M., Jalkanen, S., Johnson, M. S., and Salminen, T. A. (2005) Crystal structure of the human vascular adhesion protein-1: Unique structural features with functional implications. *Protein Sci.* 14, 1964–1974.
 16. Chiu, Y.-C., Okajima, T., Murakawa, T., Uchida, M., Taki, M., Hirota, S., Kim, M., Yamaguchi, H., Kawano, Y., Kamiya, N., Kuroda, S., Hayashi, H., Yamamoto, Y., and Tanizawa, K. (2006) Kinetic and structural studies on the catalytic role of the aspartic acid residue conserved in copper amine oxidase. *Biochemistry* 45, 4105–4120.
 17. Matsuzaki, R., Fukui, T., Sato, H., Ozaki, Y., and Tanizawa, K. (1994) Generation of the topa quinone cofactor in bacterial monoamine oxidase by cupric ion-dependent autooxidation of a specific tyrosyl residue. *FEBS Lett.* 351, 360–364.
 18. Scaman, C. H., and Palcic, M. M. (1992) Stereochemical course of tyramine oxidation by semicarbazide-sensitive amine oxidase. *Biochemistry* 31, 6829–6841.
 19. Günther, H., Alizade, M. A., Kellner, M., Biller, F., and Simon, H. (1973) Biochemical synthesis of stereospecifically hydrogen labeled compounds on a preparative scale, V1–3. Preparation of (1R) (1-²H)- and (1S) (1-²H)-alcohols by exchange reactions catalyzed by yeast or a coupled enzyme system. *Z. Naturforsch.* C28, 241–246.
 20. Mitsunobu, O., and Yamada, M. (1967) Preparation of esters of carboxylic and phosphoric acid via quaternary phosphonium salts. *Bull. Chem. Soc. Jpn.* 40, 2380–2382.
 21. Leslie, A. G. W. (1992) *Joint CCP4 and EESF-EACMB Newsletter on Protein Crystallography*, SERC Daresbury Laboratory, Warrington, U.K.
 22. Collaborative Computational Project Number 4 (1994) The CCP 4 suite: programs for protein crystallography. *Acta Crystallogr. D50*, 760–763.
 23. Brünger, A. T., Adams, P. D., Clore, G. M., DeLano, W. L., Gros, P., Grosse-Kunstleve, R. W., Jiang, J. S., Kuszewski, J., Nilges, M., Pannu, N. S., Read, R. J., Rice, L. M., Simonson, T., and Warren, G. L. (1998) Crystallography & NMR system: A new software suite for macromolecular structure determination. *Acta Crystallogr. D54*, 905–921.
 24. McRee, D. E. (1999) XtalView/Xfit: A versatile program for manipulating atomic coordinates and electron density. *J. Struct. Biol.* 125, 156–165.
 25. Kleywegt, G. J., and Jones, T. A. (1997) Model building and refinement practice. *Methods Enzymol.* 277, 208–230.
 26. Prabhakaran, P. C., Gould, S. J., Orr, G. R., and Coward, J. K. (1988) Synthesis of chirally deuterated phthalimidopropanols and evaluation of their absolute stereochemistry. *J. Am. Chem. Soc.* 110, 5779–5784.
 27. Murakawa, T., Okajima, T., Taki, M., Yamamoto, Y., Kuroda, S., Hayashi, H., and Tanizawa, K. (2006) Quantum mechanical hydrogen tunneling in bacterial copper amine oxidase reaction. *Biochem. Biophys. Res. Commun.* 342, 414–423.
 28. Kleywegt, G. J., and Jones, T. A. (1994) Detection, delineation, measurement and display of cavities in macromolecular structures. *Acta Crystallogr. D50*, 178–185.

BI800623F